New analysis of $p + {}^{19}$F reactions at low energies and the spectroscopy of natural-parity states in ^{20}Ne

Ivano Lombardo,[1,*] Daniele Dell'Aquila,[1,2,†] Jian-Jun He,[3,‡] Giulio Spadaccini,[4,5] and Mariano Vigilante[4,5]

[1]*INFN, Sezione di Catania, Via Santa Sofia, I-95126 Catania, Italy*

[2]*Ruđer Bošković Institute, Bijenička cesta 54, 10000 Zagreb, Croatia*

[3]*Key Laboratory of Beam Technology of Ministry of Education, College of Nuclear Science and Technology, Beijing Normal University (BNU), Beijing 100875, China*

[4]*INFN, Sezione di Napoli, Via Cintia, I-80126 Napoli, Italy*

[5]*Dipartimento di Fisica "E. Pancini," Università di Napoli Federico II, Via Cintia, I-80126 Napoli, Italy*

(Received 28 May 2019; revised manuscript received 9 August 2019; published 10 October 2019)

Low-spin natural-parity states in ^{20}Ne at excitation energies larger than the proton separation energy can be fruitfully explored by analyzing the behavior of the ^{19}F$(p,\alpha_0)^{16}$O and ^{19}F$(p,\alpha_\pi)^{16}$O reactions. Previous analyses were affected by the presence of fragmentary data, often limited to small bombarding energy ranges and to just one reaction channel, preventing any firm conclusion on the spectroscopy of such states. We propose a critical analysis of all data sets published in the literature, especially concerning angular distribution and cross-section data of the ^{19}F$(p,\alpha_0)^{16}$O and ^{19}F$(p,\alpha_\pi)^{16}$O reactions at low bombarding energies ($E_p \approx 0.2$–10 MeV). For the first time, we perform a comprehensive R-matrix analysis of all such data, including also $p+{}^{19}$F elastic scattering data to better determine the partial widths associated to each decay channel. The obtained results help to remove uncertainties on several J^π assignments for known states and point out the possible non-negligible role played by low-energy resonances in the determination of the ^{19}F$(p,\alpha_\pi)^{16}$O reaction rate at temperatures relevant for Asimptotic Giant Branch (AGB) stars.

DOI: 10.1103/PhysRevC.100.044307

I. INTRODUCTION

The study of proton-induced nuclear reactions on ^{19}F is a very powerful tool to probe the spectroscopy of the self-conjugate ^{20}Ne nucleus at excitation energies larger than the proton separation energy, i.e., $S_p = 12.844$ MeV [1]. At proton bombarding energies of few hundreds keV, several reaction channels are already energetically open: the elastic scattering channel, the inelastic scatterings to the first and the second excited states in ^{19}F ($E_x = 107$ keV and $E_x = 191$ keV, respectively), the ^{19}F$(p,\alpha_0)^{16}$O ($Q = 8.114$ MeV) reaction, the ^{19}F$(p,\alpha_\pi)^{16}$O (E_x in ^{16}O $= 6.05$ MeV) reaction, and the group of α transmutations followed by high-energy γ-ray emission: ^{19}F$(p,\alpha_\gamma)^{16}$O (E_x in ^{16}O $= 6.13, 6.92, 7.12$ MeV) [1,2]. The radiative capture reaction ^{19}F$(p,\gamma)^{20}$Ne is open but, on the average, it has a cross section well smaller than the other reaction channels [3]. Because of angular momentum and parity conservations in nuclear forces, only natural-parity states of ^{20}Ne can decay in the α_0 and α_π channels [4,5]. At variance, both natural- and unnatural-parity states can decay in all the other reaction channels listed above. This selectivity, coupled with relatively low orbital angular momenta involved at low $E_{\text{c.m.}}$ values, makes this reaction a powerful tool to study the spectroscopy of ^{20}Ne at $E_x > 12.844$ MeV.

The accumulation of ≈80 years of data now allows for a more global analysis, which can add better constraints on the spectroscopy of excited states in ^{20}Ne than each measurement taken individually; indeed, in Ref. [1], where all the published results were collected and critically reviewed, it is quite frequent to see the presence of tentative states, or with uncertain J^π assignments, or without any quoted partial decay width. A possible way to improve this situation should proceed via a comprehensive analysis of a broad and validated data set involving all the reactions here discussed.

In this respect, it is interesting to note a recent effort, made by our experimental group and others, in the reanalysis of a broad body of data on differential cross sections of elastic scattering channel at several angles [6,7] and of differential and angle-integrated cross section of the ^{19}F$(p,\alpha_0)^{16}$O reaction [8–11]. In this paper, for the first time, we perform an extended and comprehensive R-matrix analysis including all such data, coupled with available data on the ^{19}F$(p,\alpha_\pi)^{16}$O reaction. As will be shown in the paper, including the ^{19}F$(p,\alpha_\pi)^{16}$O data in the analysis is a crucial ingredient to more firmly constrain the spectroscopy of ^{20}Ne above proton separation energy. Our analysis clarifies several ambiguities in the spectroscopy of natural-parity states in ^{20}Ne. The phases of data selection and data analysis via R-matrix fit are described, respectively, in Secs. II and III.

Since ^{19}F$(p,\alpha)^{16}$O reaction is also involved in the fluorine nucleosynthesis in Asimptotic Giant Branch (AGB) stars, the presence of low-energy states, and the knowledge of their spectroscopy in ^{20}Ne, is important to judiciously estimate the

*ivano.lombardo@ct.infn.it

†daniele.dellaquila@irb.hr

‡hejianjun@bnu.edu.cn

reaction rate at low temperature by means of reliable extrapolations. In Sec. IV, we discuss the impact of the presence of a nonvanishing Γ_{α_π} partial decay width of the 13.095-MeV state in the low temperature regime of the ^{19}F$(p,\alpha_\pi)^{16}$O reaction rate.

II. DISCUSSION OF AVAILABLE EXPERIMENTAL DATA

In recent times, we published a comprehensive reanalysis of the ^{19}F$(p,\alpha_0)^{16}$O angle-integrated cross-section data [10]. The comparison of several data sets, and the presence of overlapping regions between them, allowed us to critically disentangle the behavior of the cross section and the presence of relative normalizations factors. In this way, we were able to evaluate the ^{19}F$(p,\alpha_0)^{16}$O angle-integrated cross section in the proton bombarding energy range $E_{\rm lab} \simeq 0.18$–3.35 MeV. If we include in this systematics also the high-energy data of Warsh *et al.* [12], we can enlarge the bombarding energy domain up to $E_{\rm lab} \approx 12.3$ MeV. This is an important aspect, since at these high energies the main contribution to the cross section comes from direct processes, triggered by the cluster structure of ^{19}F in terms of $t + {}^{16}$O and $\alpha + {}^{15}$N configurations [19–21]. However, as pointed out by many authors [9,22,23], such direct processes appear also at sub-Coulomb energies and influence the trend and absolute value of the S factor at low energies. Despite experimental and theoretical efforts, the literature reports conflicting estimates of the shape and magnitude of the direct component of the S factor at low energies [10,22–24]. Therefore, the analysis of high-energy data could help us to better understand the behavior of the direct term of the S factor at low energies.

Together with the ^{19}F$(p,\alpha_0)^{16}$O reaction, also the ^{19}F$(p,\alpha_\pi)^{16}$O reaction is of fundamental importance to the study of natural-parity states in ^{20}Ne [1]. Unfortunately, regarding this reaction, available experimental cross-section data are quite limited, and they are often conflicting, as pointed out by the NACRE Collaboration [25]. The available data sets include the data reported by Devons *et al.* [15] and by Ranken *et al.* [26], which made use of pair spectrometer, and by Caracciolo *et al.* [16] and Cuzzocrea *et al.* [13], which made use of high-resolution solid-state detectors to identify the peak associated with the α_π ejectile.

Apart from the data reviewed by NACRE, some other (partial) data sets also exist. In very old works, Streib *et al.* [27] reported a yield curve in the $E_p = 0.4$–1.4 MeV domain, while Phillips and Heydenburg [28] reported an excitation function in arbitrary units, in the $E_p = 0.8$–2 MeV range. Isoya *et al.* [29] reported an excitation curve (without experimental points) for the ^{19}F$(p,\alpha_\pi)^{16}$O at $E_p = 0.6$–1.5 MeV; the absolute cross-section scale was determined by comparison with the ^{19}F$(p,\alpha_\gamma)^{16}$O cross-section values by Chao *et al.* [30]. Finally, Ouichaoui *et al.* [18,31] reported excitation functions in absolute units at backward angles by detecting α_π ejectiles with solid-state detectors.

To derive a coherent dataset describing the ^{19}F$(p,\alpha_\pi)^{16}$O cross section as a function of energy, we decided to assume as a reference the data obtained by detecting the α_π ejectile with high-resolution solid-state detectors, i.e., the ones of Refs. [13,16,34]: They are not affected by uncertainties on efficiency estimates and by possible contaminations from the α_γ channels that usually characterize the use of electron-positron detectors.

Furthermore, the independent measurement of differential cross sections for the α_π by Ouichaoui *et al.* [18,31] shows results in good agreement with the ones of Refs. [13,34]. The shape of the data by Devons *et al.* [15] at $E_{\rm lab} < 1.1$ MeV is in good agreement with the one reported by Caracciolo *et al.* [16], but the absolute cross section is larger by a factor of 2. Therefore, we normalized by a factor 0.5 the data of Ref. [15]. We expunged from the Devons *et al.* data some spikes that are clearly due to contaminations of α_γ channels; such spikes were absent in the Isoya excitation curve of Ref. [5]. We exclude from the dataset the highest energy points of Ref. [15] ($E_{\rm lab} > 1.1$ MeV); once normalized by a factor 0.5 (as for the low-energy points), their absolute values disagree with the ones reported in Ref. [5], possibly because of efficiency problems. By using the data coming from Refs. [13,15,16,34], we cover the regions $E_{\rm lab} = 0.6$–1.1 MeV and 1.7–2.5 MeV. A lack of data in the region 1.1–1.7 MeV would make the analysis uncertain.

Luckily, in Ref. [17], which is a report of all the data coming from the experimental campaign that lead to the publications of Refs. [13,16,34], performed at the CN accelerator in Legnaro, Italy [35], and at the TTT3 tandem accelerator in Naples, Italy [36–40], the authors discuss and show the results of measurements in the domain $E_{\rm lab} = 0.7$–1.7 MeV. Such results have been obtained with the same experimental techniques used in Refs. [13,16,34]. They report absolute angle-integrated cross sections for the ^{19}F$(p,\alpha_\pi)^{16}$O reaction near the $E_{\rm lab} = 1.12$ and 1.36 MeV resonances, as determined from detailed angular distribution measurements in the range $\theta_{\rm lab} = 45$–155°; we included such data in our dataset for this reaction channel. In the same Ref. [17], the authors report also excitation functions in absolute units for the ^{19}F$(p,\alpha_\pi)^{16}$O reaction at $\theta_{\rm lab} = 85, 95, 105, 115, 125, 135, 145, 155^\circ$, with data points that cover also the region between these two resonances (i.e., $E_{\rm lab} \approx 1.16$–1.32 MeV). We complemented our database in this region by calculating the angle integrated cross section via the experimental points of the absolute differential cross sections of Ref. [17] and assuming the angular distribution shapes reported in this energy region in Ref. [29]. The agreement between the angular trend of data from Ref. [17] and the shape of angular distributions of Ref. [29] is very good at all the energies. The estimated overall uncertainty in the cross section is about 15%.

To reasonably determine the partial width for each excited state in ^{20}Ne, it is fundamental to reproduce consistently all the excitation functions for each open decay channel. In particular, it is important to carefully reproduce the trend of elastic scattering excitation functions, in the largest possible angular range. In recent times, many authors (see, e.g., Refs. [6,7]) discussed and reviewed available experimental data sets of ^{19}F$(p,p_0)^{19}$F elastic scattering in the energy domain $E_{\rm lab} \approx 0.5$–6.0 MeV, pointing out some normalization problems between them. In the lowermost energy range, the data of Caracciolo *et al.* [16] are in very good agreement

with those of Webb *et al.* [41]; the highest energy data points by Webb are furthermore in good agreement with the benchmarked data by Paneta *et al.* [6]. We used the Caracciolo et al excitation functions at $\theta_{\rm lab} = 135^\circ, 145^\circ$ to better determine the decay partial widths of excited states. In the *R*-matrix fit procedure described in the next section, we allowed the presence of a global normalization factor (within 5% of the absolute cross-section values), as a free parameter to take into account possible (small) normalization errors in the elastic differential cross sections.

When a proton beam collides against a ^{19}F target, there are other open reaction channels besides the ones above discussed: the ^{19}F$(p,\gamma)^{20}$Ne radiative capture, the ^{19}F$(p,p')^{19}$F inelastic scattering (with an energy threshold of 116 keV when the first excited state of ^{19}F is involved), and the already mentioned ^{19}F$(p,\alpha_\gamma)^{16}$O (feeding the 6.13-, 6.93-, 7.13-MeV excited states in ^{16}O). Analogously to the elastic scattering case, excited states in ^{20}Ne with both natural and unnatural parities can form resonances in the cross section of such reaction channels. In the present analysis, for simplicity, we did not include data related to the ^{19}F$(p,\gamma)^{20}$Ne radiative capture channel that shows cross-section values much smaller than all the other reaction channels in the whole energy range [3,25]. Furthermore, looking at the Tables 20.26 and 20.29 of Ref. [1] and to Ref. [2], it seems that for inelastic and α_γ reaction channels the dominating resonances are mainly due to unnatural-parity states. To avoid an excessive complication, we did not include experimental data of such reaction channels in the fit procedure, but we used as a guideline the trend of experimental data of angle-integrated inelastic scattering cross section shown in Ref. [42], together with the previously reported values of the partial widths (where quoted) of Tables 20.26 and 20.29 [1].

We neglected the contribution given by the reaction ^{19}F$(p,{}^8\,\mathrm{Be})^{12}$C ($Q = +0.86$ MeV) because, at low energies, it has a phase-space factor lower and a Coulomb barrier higher than the $\alpha + {}^{16}$O channel, and this would suppress the $\Gamma_{^8\mathrm{Be}}$ partial widths for excited states populated in low-energy experiments. To our knowledge, the only existing experiment on the ^{19}F$(p,{}^8\,\mathrm{Be})^{12}$C reaction was made at high bombarding energy ($E_p \approx 2.7$–5.7 MeV) by Gorodetzky *et al.* [43], in connection with the study of quartet excitations in self-conjugated nuclei [44,45], and even for states at large excitation energies ($E_x > 15.4$ MeV) the reported ^{8}Be branching ratios are typically quite small.

The large body of data reported in the literature on $\alpha + {}^{16}$O elastic and inelastic scattering has allowed us to obtain details on the Γ_α partial widths of excited states in ^{20}Ne (see, e.g., Ref. [46]). In our work, we often refer, as a comparison, to the results obtained in $\alpha + {}^{16}$O elastic scattering experiments at high energies described by Caskey [47] ($E_\alpha = 9.2$–13.5 MeV) and Metha *et al.* [48] ($E_\alpha = 10$–19 MeV), and to the inelastic scattering (to the first excited state in ^{16}O) experiment by Laymon *et al.* [49] ($E_\alpha = 10.2$–18 MeV).

Finally, a comprehensive revision of all the datasets available in the literature for the ^{19}F$(p,\alpha\gamma)^{16}$O reaction is currently ongoing, and its analysis would be useful for a future, more detailed, collateral analysis on unnatural parity states in ^{20}Ne.

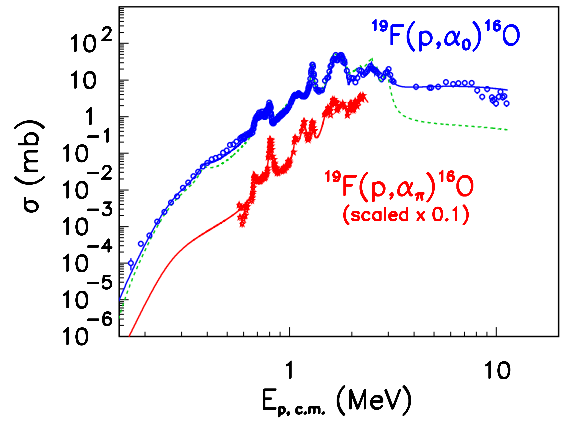

FIG. 1. Cross sections of the ^{19}F$(p,\alpha_0)^{16}$O (blue circles) and ^{19}F$(p,\alpha_\pi)^{16}$O (red stars, scaled by a factor 0.1 for clarity reasons) reactions, as a function of the center of mass energy. Solid lines represent the result of the comprehensive *R*-matrix fit of data, as discussed in the text. The green dashed line shows the result of the *R*-matrix fit without including the direct contribution parameterized as discussed in the text.

III. *R*-MATRIX FIT OF DATA

The experimental angle-integrated cross section data for the ^{19}F$(p,\alpha_0)^{16}$O (shortened as α_0) and ^{19}F$(p,\alpha_\pi)^{16}$O (shortened as α_π) reactions and the differential cross sections of the ^{19}F$(p,\mathrm{p}_0)^{19}$F scattering (shortened as p_0) are shown as points with error bars in Figs. 1–4 (Table I). They have been simultaneously fitted by using the *R*-matrix code AZURE2 [50–52]. This type of *R*-matrix analysis of cross-section data is widely used in the literature to improve the spectroscopy of excited states formed in compound nucleus experiments [46,53]. We used channel radii given by the formula $R = 1.4(A_1^{1/3} + A_2^{1/3})$ fm, where A_1 and A_2 are the mass numbers of the nuclei in each channels. In our analysis, we adopted the Brune formalism [54]. As input values for the resonance parameters, we adopted the ones reported in Ref. [1]. Concerning the analysis of natural-parity states that de-excite via the α_0 and α_π channels, it has been widely discussed in the literature [5,8,9,11,14,16,55,56] that the analysis of angular

TABLE I. List of experimental data used in the present analysis (integrated cross section, differential cross section, angular distributions). The energy values are expressed in the laboratory frame.

Reaction channel	Data type	Energy range (MeV)	Ref.
^{19}F$(p,\alpha_0)^{16}$O	Int. cross sect.	0.18–3.35	[10]
^{19}F$(p,\alpha_0)^{16}$O	Int. cross sect.	4.3–12.3	[12]
^{19}F$(p,\alpha_0)^{16}$O	Ang. distr.	2.12–2.62	[13]
^{19}F$(p,\alpha_0)^{16}$O	Ang. distr.	2.72–3.13	[14]
^{19}F$(p,\alpha_\pi)^{16}$O	Int. cross sect.	0.6–1.05	[15]
^{19}F$(p,\alpha_\pi)^{16}$O	Int. cross sect.	0.79–0.87	[16]
^{19}F$(p,\alpha_\pi)^{16}$O	Int. cross sect.	1.1–1.38	[17]
^{19}F$(p,\alpha_\pi)^{16}$O	Int. cross sect.	1.55–2.38	[13]
^{19}F$(p,\alpha_\pi)^{16}$O	Diff. cross sect.	2.72–2.8	[18]
^{19}F$(p,\alpha_\pi)^{16}$O	Ang. distr.	2.06–2.18	[13]
^{19}F$(p,\mathrm{p}_0)^{19}$F	Diff. cross sect.	0.66–1.8	[16]

distributions in terms of Legendre or cosine polynomials is useful to determine the relative orbital angular momentum ℓ of the outgoing channel and, consequently, of the J^π of the excited state. Taking into account such a point, we used in our R-matrix fit the J^π values of natural-parity states according to the angular distributions analyses discussed in the literature (and partially collected in Ref. [1]): In the range $E_{\rm lab} \approx 0.2$–0.6 MeV from Refs. [9,55], in the range $E_{\rm lab} \approx 0.6$–0.9 MeV from Refs. [2,5,8,16,55], in the range $E_{\rm lab} \approx 0.9$–1.3 MeV from Refs. [2,5], in the range $E_{\rm lab} \approx 1.3$–1.5 MeV from Refs. [2,33], in the range $E_{\rm lab} \approx 1.5$–2.5 MeV from Refs. [13,14,33,34], and finally in the range $E_{\rm lab} \approx 2.5$–3.3 MeV from Refs. [14]. Where ambiguities are present in the literature, we tried to solve them by a dedicated analysis of excitation functions or of angular distributions taken from the datasets listed above.

The starting values of resonance parameters for the unnatural-parity states that contribute in the differential cross section of the p_0 elastic scattering data here analyzed are taken from Ref. [1], taking into account also specific findings reported in Refs. [2,7,18,31,41] that were related to the analysis of states involved in elastic scattering.

Since, as discussed in the previous sections, for the α_0 channel the presence of direct effects has been reported both at high [19,20] and low [9,22,25] energies, we included two very broad poles in s-wave and p-wave at $E_x = 23$ MeV having nonvanishing Γ_{α_0} and Γ_{p_0} partial widths. The inclusion of high-energy data in our database allows us to reasonably determine such a direct contribution; its effect on the high-energy part of the integrated cross section is clearly visible in Fig. 1, where the green dashed line would represent the result of the R-matrix fit without including such a direct term. It is displayed with a green dashed line also in Fig. 2 as an S factor; its trend and magnitude at low energies ($E_{\rm c.m.} < 0.8$ MeV) are quite similar to the ones obtained by using a finite-range distorted-wave Born approximation (FR-DWBA) approach in Ref. [23]. Furthermore, we verified also that the angular distributions of the simulated direct contribution at low energies are forward peaked and that they are in reasonable agreement with the ones estimated with the FR-DWBA model [23]. It is worth noting that the direct contribution quoted in Ref. [9] includes also low-energy tails of high-energy resonances.

The results of the comprehensive R-matrix fit for all the datasets here analyzed (Tables II and III) are shown as solid lines all along Figs. 1–7. The overall agreement between the R-matrix analysis and experimental data is quite satisfactory, also in consideration of the huge complexity of ^{20}Ne level scheme in such high-energy region. Depending on the reaction channel, the reduced χ^2 ranges from $\approx$1 up to $\approx$6. To estimate, on average, the uncertainty associated to our fit parameters, we used a procedure similar to the one described in Ref. [39]. With this procedure, we quote an average indetermination of 25% for the obtained widths. In the next subsections, we will discuss in more details the spectroscopic characteristics of excited states in ^{20}Ne as determined from the present analysis. In particular, the explored energy range is divided into five regions. For each region, we individually discuss the contribution of natural-parity states in the α_0, α_π, and p_0 channels. We discuss separately the contribution, due to unnatural-parity states, in the elastic scattering channel.

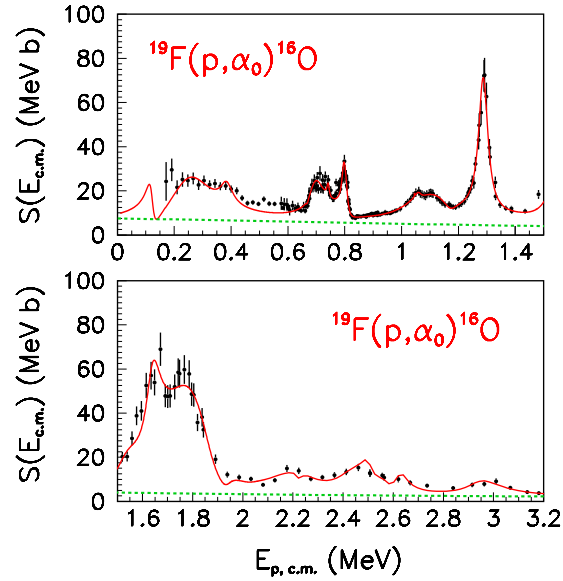

FIG. 2. S factor of the ^{19}F$(p, \alpha_0)^{16}$O reaction as a function of the center-of-mass energy. Data are taken from Refs. [10,12]. For clarity reasons, data have been split into two different energy windows. The red solid line represents the result of the comprehensive R-matrix fit of data, as discussed in the text. The green dashed line shows the trend of the direct contribution alone, parameterized as discussed in the text.

A. Resonances in the $E_{\rm c.m.} = 0.0$–0.7 MeV region

At near-zero energies, the only existing experimental data concern the α_0 channels [9]. A broad bump is seen in the S factor at $E_{\rm c.m.} \simeq 0.265$ MeV, with a long asymmetric tail extending up to 0.5 MeV. As discussed in detail in Ref. [9], this trend is due to the contribution of the $E_x = 13.095$ MeV 2^+ excited state in ^{20}Ne. The long tail was attributed to the interference of the 13.095-MeV state with another 2^+ state in close vicinity to the threshold, the 12.957-MeV 2^+ state. The contribution of this state has been predicted with indirect experiments with the Trojan horse method [57–60], while a direct measurement is planned for the future at the JUNA facility [61,62]. For the 12.957-MeV state, the resonance parameters were fixed to the values determined with the indirect technique.[1]

Concerning the 2^+ state at $E_x = 13.095$ MeV, a good description of the right tail of the bump seen in the α_0 data is obtained by using the values of total and partial width parameters quoted in Ref. [49] taken at the maximum boundaries. It is interesting to observe that in a detailed analysis of the ^{16}O$(\alpha, \alpha_\pi)^{16}$O cross section, Laymon *et al.* [49] quoted a nonvanishing partial width for the decay of such state in the α_π channel, $\Gamma_{\alpha_\pi} = 40.4 \pm 3.3$ keV. This value amount to about

[1]There is a misprint in Ref. [58] concerning the Γ_{p_0} partial width: $\gamma_{p_0} = 0.110$ MeV$^{1/2}$ corresponds to $\Gamma_{p_0} \simeq 9.8 \times 10^{-7}$ eV.

TABLE II. List of natural-parity states contributing to the $^{19}F(p,\alpha_0)^{16}O$ and $^{19}F(p,\alpha_\pi)^{16}O$ reaction cross section. The first three columns indicate the excitation energy, spin parity, and total width of states reported in the literature. Superscripts are referred to the following references: [a]Ref. [1] Table 20.17; [b]Ref. [1], Tables 20.27 and/or 20.28; [c]Ref. [8]; [d] Ref. [32]; [e]Refs. [18,31]; [f][13]; [g]Ref. [33]; [h]Ref. [14]. The last seven columns report resonance parameters determined from the present R-matrix analysis. $\Gamma_{\rm cm}$, Γ_{α_0}, and Γ_{α_π} values are expressed in keV.

E_x lit.	J^π lit.	$\Gamma_{\rm c.m.}$ lit.	E_x	J^π	$\Gamma_{\rm c.m.}$	Γ_{α_0}	Γ_{α_π}	Γ_{p_0}	$\Gamma_{p_{ine}}+\Gamma_{\alpha\gamma}$
12.957[a]	2^+	38	12.957	2^+	38	38		9.8×10^{-7} eV	
13.095[a]	2^+	162	13.095	2^+	177	133	43.7	0.036 eV	
13.226[a]	3^-	53	13.226	3^-	53	53		0.08 eV	
13.461[a]	1^-	195	13.465	1^-	214	196	18	12.43 eV	
13.522[b]	(1^-)	33	13.515	1^-	17	2.4	15	1.83 eV	
13.544[b]	2^+	63	13.541	2^+	71	64	7	13.39 eV	
13.586[b]	2^+	9	13.586	2^+	10	1	0.4	16.45 eV	9 keV
≈13.628[c]	1^-	≈30	13.632	1^-	31	30	1	4.71 eV	
13.648[b]	$(0^+,2^+)$	17	13.649	0^+	23	0.055	0.058	22.7 keV	50 eV
13.885[d]	2^+	0.8	13.885	2^+	0.8			30 eV	765 eV
≈13.87[b]	1^-	≈190	13.888	1^-	293	162	17	447 eV	114 keV
13.907[b]	2^+	48	13.910	2^+	29	8	21	21 eV	
13.950[b]	0^+	≈67	13.912	0^+	251	251		381 eV	
14.021[b]	1^-	≈67	14.02	1^-	61	6	55	189 eV	
14.130[b]	2^+	34	14.131	2^+	39	33	6	405 eV	
14.417[b]	1^-	86	14.351	1^-	151	42	108	1.0 keV	
14.475[b]	0^+	68	14.466	0^+	96	64	25	7.0 keV	
14.597[b]	1^-	116	14.596	1^-	287	212	65	9.8 keV	
14.653[b]	0^+	24	14.653	0^+	160	143	11	6.5 keV	
14.773[e]	1^-	66	14.809	1^-	94	21	71	2.1 keV	
14.85[b]	$(2,4)^+$	71	14.844	4^+	139	139		155 eV	
14.85[b]	$(2,4)^+$	71	14.854	2^+	109	4	105	64 eV	
14.92[b,f]	0^+	40	14.919	0^+	39		37	1.9 keV	
15.04[b]	(2^+)	86	15.061	2^+	68	17	49	1.8 keV	
15.05[e]	2^+	29	15.118	2^+	208	36	166	6.4 keV	
15.31[b,g]	(0^+)	285	15.297	0^+	204	20	2	173 keV	9.3 keV
15.34[e]	2^+	57	15.327	2^+	680	101	169	0.7 keV	409 keV
15.27[b]	(1^-)	285	15.350	1^-	61	6	1	16 keV	38 keV
15.39[b]		76	15.419	2^+	60	29	29	63 eV	1.7 keV
15.44[b]		57	15.451	3^-	45	32	13	40 eV	
15.53[b]		152	15.590	2^+	709	113	81	2.7 keV	512 keV
(15.64)[b]			15.617	0^+	185	5	163	0.4 keV	17 keV
(15.81)[b]		162	15.803	1^-	186	17	0.2	13.5 keV	155 keV
15.88[h]	(3^-)	138	15.821	3^-	205	204		1.0 keV	

TABLE III. List of unnatural-parity states introduced to describe (together with the natural-parity ones) the differential cross section of the $p+{}^{19}$F elastic scattering at backward angles. The first three columns indicate the excitation energy, spin parity, and total width of each state as reported in the literature. Superscripts are referred to the following references: [a]Ref. [1], Table 20.25; [b]Ref. [1], Table 20.26; [c]Ref. [31]. Total and partial widths are expressed in keV.

E_x lit.	J^π lit.	$\Gamma_{\rm c.m.}$ lit.	E_x	J^π	$\Gamma_{\rm c.m.}$	Γ_{α_0}	Γ_{α_π}	Γ_{p_0}	$\Gamma_{p_{ine}+\alpha\gamma}$
13.483[a]	1^+	7.1	13.479	1^+	7.1			7.1	0.283
13.677[a]	2^-	4.9	13.675	2^-	4.6			0.82	3.76
13.736[a]	1^+	7.0	13.730	1^+	9.8			3.1	6.7
13.928[b]		3.5	13.915	1^+	4.2			1.0	3.2
14.03[b]		≈76	14.03	1^+	74			1.0	73
14.126[a]	2^-	4.3	14.126	2^-	4.7			0.6	4.1
14.151[a]	2^-	14	14.151	2^-	15			4.8	10.2
14.198[a]	1^+	13.9	14.195	1^+	17.2			12	5.2
14.452[c]	$(1^-,2^-)$	27	14.45	2^-	20			0.55	19.5
14.691[c]	(1^+)	38	(14.71)	(1^+)	(220)			(100)	(120)

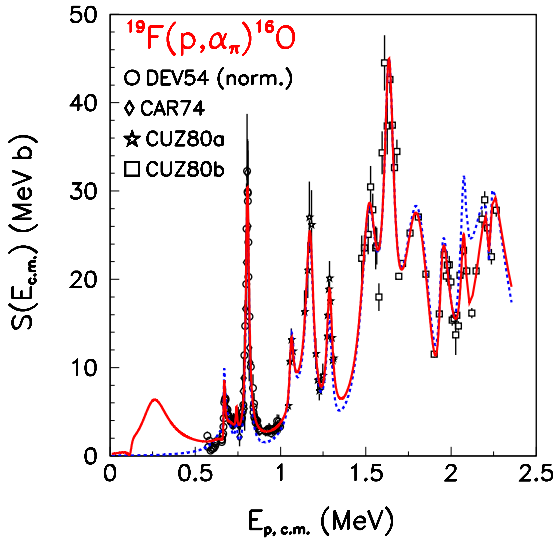

FIG. 3. S factor of the ^{19}F$(p,\alpha_\pi)^{16}$O reaction as a function of the center-of-mass energy. Data coming from different works are indicated by different symbols: open circles (DEV54 norm), Ref. [15]; open diamonds (CAR74), Ref. [16]; open stars (CUZ80a), Ref. [17]; and open squares (CUZ80b), Ref. [13]. The red solid line represents the result of the comprehensive R-matrix fit of data, as discussed in the text. The blue dashed line shows the trend of the R-matrix fit assuming zero partial width for the 13.095-MeV 2^+ state.

70% of the Wigner limit, pointing out a strong α clusterization for this state. If we include such a branching at the maximum boundary in the R-matrix calculation of the α_π channel (i.e., $\Gamma_{\alpha_\pi} = 43.7$ keV), a strong increase of the S factor at very low energies ($E_{\rm c.m.} \approx 0.26$ MeV) is clearly seen (red solid line in Fig. 3) if compared with calculations assuming no α_π decay branch for this state (blue dotted line in Fig. 3). The effect of the 13.095-MeV state in the reaction rate calculation for the α_π channel will be discussed in detail in Sec. IV. It is noteworthy that a digitization of the very old α_π data by Streib *et al.* [27] reveals, in this energy region, a resonant-like trend of the S factor in qualitative agreement with the hypothesis made in the present work.

The small anomaly at $E_{\rm c.m.} \approx 0.38$ MeV is associated with the 3^- state at $E_x = 13.226$ MeV, as seen also with the Trojan horse method [58,60]. At higher energies, a broad 1^- state at $E_x = 13.465$ MeV is needed to reproduce in the best possible way the S-factor data for the α_0 channel in the $E_{\rm c.m.} \approx 0.52$–$0.58$ MeV region and to explain also the dip seen at $E_{\rm c.m.} \approx 0.83$ MeV. The $\Gamma_{\rm tot}$ value obtained from the fit is 214 keV, very close to the one reported in the literature (195 keV, [1,47,55]); also the quoted branching $\frac{\Gamma_{\alpha_0}}{\Gamma_{\rm tot}} \simeq 0.92$ is similar to the one of Ref. [47]. Probably, a better agreement between the fit and experimental α_0 channel data could be obtained by including a narrow resonance at $E_{\rm c.m.} \approx 0.514$ MeV and one or two broader resonances in the region $E_{\rm c.m.} \approx 0.54$–$0.64$ MeV. However, the limited number of data points in such energy window for the α_π channel prevents a similar analysis and calls for new experimental data.

B. Resonances in the $E_{\rm c.m.} = 0.7$–1.0 MeV region

The α_π channel data show a narrow peak at $E_{\rm c.m.} = 0.676$ MeV that is associated with a state at $E_x = 13.515$ MeV. The existence of a tentatively assigned 1^- state at a very similar energy (13.522 MeV) was suggested in Ref. [5], where an upper limit was given for the Γ_{α_0} partial width. Signals of the existence of such a state were found also by studying the ^{16}O$(\alpha,\alpha_0)^{16}$O and ^{16}O$(\alpha,\alpha_\pi)^{16}$O reactions [47,63], with a dominance of the α_π branching. Parameters derived from the present analysis agree reasonably well with previous ones. Furthermore, we checked the possibility of having alternative 0^+ or 2^+ assignments for such a resonance; if we use a 0^+ or 2^+ assignment, we observe a poorer description of data concerning the steep rise in the left part of the resonance in the α_π channel if compared to the 1^- case.

At slightly higher energies, two 2^+ resonances occur: They are due to excited states at $E_x = 13.541$ and 13.586 MeV. The first is responsible for the peak at $E_{\rm c.m.} \approx 0.7$ MeV in the α_0 channel, while the second appears as a narrow (and small) peak in both α_0 and α_π channels at $E_{\rm c.m.} \simeq 0.742$ MeV. Angular distribution analyses lead to certain 2^+ assignments for both states [5,8,55]. The partial widths here reported for the 13.541-MeV state agree well with values of Ref. [5]; the $\frac{\Gamma_{\alpha_0}}{\Gamma_{\rm tot}}$ branching ratio is not far from the estimate of Ref. [47] obtained in $\alpha + ^{16}$O elastic scattering. Similar findings are obtained for the 13.586-MeV state; in this case a sizable partial width in the inelastic channel p_2 would be in agreement with experimental data of Ref. [42] and is similar to the findings of Ref. [5].

In the $E_{\rm c.m.} \approx 0.8$ MeV region, a narrow peak, preceded by a left shoulder, is seen in both the α_0 and α_π data, while a pronounced anomaly is seen in the differential cross section of $p+^{19}$F elastic scattering data. The presence of a double-humped peak is clearly visible in the α_0 and α_π cross section data of Ref. [16]. In both Refs. [8,16], the analysis of angular distributions point out the contribution of a small 1^- state at 13.632 MeV and a dominant 0^+ state at 13.649 MeV. The J^π of the latter was also suggested to be 2^+ in Ref. [5], with a very small $\Gamma_{p_0} = 48$ eV partial width. The simultaneous R-matrix analysis of scattering and reaction data here performed allows us to clarify this point. To reproduce all the datasets, we must use a 0^+ assignment for the 13.649-MeV state, in agreement with Refs. [2,8,16]. In fact, the use of the alternative 2^+ assignment would lead to a reasonable reproduction of the α_0- and α_π-channel data (with a set of partial widths similar to the one reported in Ref. [5]), but with a strong disagreement with the elastic scattering data. The fit result obtained with such choice of parameters is shown, for the elastic scattering data, in the inserts of Fig. 4 with the blue dashed lines.

In our analysis, we have not found signals of the two broad states, suggested in Ref. [5], at $E_{\rm lab} \approx 0.86$ and 0.93 MeV ($E_x \approx 13.66$ and 13.73 MeV). Both were predicted to have nearly 100% α_0 partial width, but the 13.66-MeV state was not seen in the $\alpha + ^{16}$O analysis of Ref. [47], while a 13.741-MeV 0^+ state was seen in Ref. [47], but with a much smaller total width and a much lower Γ_{α_0} partial width. A new experiment focused on this energy region could shed light on the existence

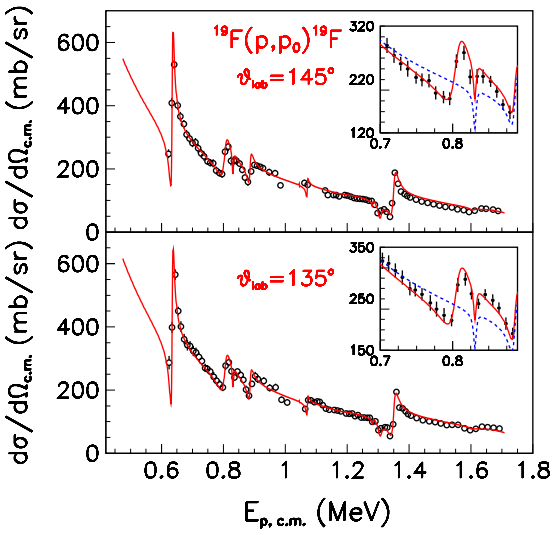

FIG. 4. Differential cross section of p+^{19}F elastic scattering at polar angles in the laboratory frame 145° and 135°. Data are taken from Ref. [16]. The red solid lines represent results of the comprehensive R-matrix fit of data, as discussed in the text. In the two inserts, blue dashed lines show the trend of the R-matrix fit obtained by assuming a 2^+ assignment for the 13.649-MeV state.

or influence of such states in the presently studied reaction channels.

C. Resonances in the $E_{\text{c.m.}} = 1.0$–1.5 MeV region

The gross structure of the bump present at $E_{\text{c.m.}} \approx 1.0$–$1.18$ MeV in the α_0 data is explained by a broad 1^- state at 13.888 MeV ($\Gamma_{\text{tot}} \simeq 293$ keV). Signals of the existence of such a state, with characteristics similar to the ones here reported, are found in previous studies (e.g., Ref. [5]: $E_x = 13.87$ MeV, $\Gamma_{\text{tot}} \simeq 190$ keV, dominant α_0 branching). The two small peaks at $E_{\text{c.m.}} \simeq 1.06$ and 1.15 MeV that modulate such gross structure are due to two resonant states at $E_x = 13.91$ and 13.912 MeV, respectively. The 13.91-MeV state has a large branching in the α_π channel ($\simeq$72% in our analysis, different from the $\simeq$38% quoted in Ref. [5]), and it is clearly seen in the α_π data as a small peak at $E_{\text{c.m.}} = 1.064$ MeV. Its 2^+ assignment was determined via angular distribution analysis in Refs. [5,29]; similar results are reported in [17]. The second peak at $E_{\text{c.m.}} \simeq 1.12$ MeV is clearly visible only in the α_0 data; therefore, in agreement with Ref. [5], only nonvanishing Γ_{α_0} and Γ_{p_0} partial widths were allowed in the fit procedure. The obtained $\Gamma_{\text{tot}} \simeq 251$ keV is larger than the ones tentatively quoted in Ref. [5] ($\approx$67 keV) and in Ref. [47] from $\alpha + {}^{16}$O analysis (79 ± 15 keV). Anyway, such larger Γ_{tot} value is needed to correctly reproduce the shape and the absolute value of the dip in the S factor seen at $E_{\text{c.m.}} \approx 1.185$ MeV. The almost 100% α_0 branching is in good agreement with findings of Refs. [47] and [5], and also the 0^+ assignment is well grounded.

In this excitation energy region, also a special 2^+ state at $E_x = 13.885$ MeV has been reported in the literature [1,32]; this state has a sizable Γ_γ partial width and does not decay via α_0 and α_π channels. If included in the level scheme, it shows a very small contribution to the p+^{19}F scattering channel, appearing as a very small wing at $E_{\text{c.m.}} \simeq 1.045$ MeV in the differential cross sections of Fig. 4.

At $E_{\text{c.m.}} \approx 1.17$ MeV, a peak clearly appears in the α_π data, while no evident structures are seen in the α_0 and elastic scattering data. It is difficult to ascertain if a peak seen in the $p + {}^{19}$F inelastic scattering data to the first excited state in ^{19}F [42] at close $E_{\text{c.m.}}$ energy is due to the same natural-parity state or to a close-lying unnatural-parity state. In our analysis, we used a 1^- state at $E_x = 14.02$ MeV ($\Gamma_{\text{tot}} \simeq 61$ keV, very close to values reported in Refs. [5,47]) with a dominant α_π branching, while the broader bump seen in the inelastic scattering data at similar energies [42] is attributed to a 1^+ unnatural-parity state at 14.03 MeV. We verified that the use of a single 1^- state at 14.02 MeV fails to reproduce all the dataset well, including the inelastic scattering data of Re. [42], with the R-matrix analysis here performed.

In the present analysis, we have not found signatures of the 14.03-MeV broad 2^+ state reported in Ref. [5]. This state was only tentatively suggested in Ref. [47], but with a Γ_{α_0} partial width much smaller than the value reported in Ref. [5] (branching ratios: 24% vs $\simeq$100%). Only a dedicated analysis of detailed angular distributions in this energy region would clarify its existence.

Finally, in this region, a pronounced peak is seen at $E_{\text{c.m.}} \approx 1.29$ MeV in both α_0 and α_π data, and also a small fluctuation in elastic scattering data is present. As discussed in the literature [5,33,47], this peak is due to a 2^+ state at $E_x = 14.131$ MeV. The total width here obtained, $\Gamma_{\text{tot}} \simeq 39$ keV, is similar to values reported in the literature [1,5,33,47,64]. The quoted α_0 branching ratio ($\approx$85%) is in nice agreement with the values of Ref. [5] (90%) and of Ref. [47] (71$\pm$6%), obtained by analyzing $\alpha + {}^{16}$O elastic scattering data.

D. Resonances in the $E_{\text{c.m.}} = 1.5$–1.9 MeV region

This region is characterized by a strong, double-humped bump in the α_0 data [33,34] and a triple-humped bump in the α_π data [13,34]. As discussed in Ref. [10], in this energy region the α_0 datasets of Refs. [34] and [33] show discrepancies that lead to a more uncertain determination of resonance parameters (roughly of the order of 40% relative errors), clearly demanding for new experiments. The α_0 data used here are obtained by averaging the ones of Refs. [33,34].

The first peak seen in this energy region is at $E_{\text{c.m.}} \approx 1.53$ MeV in the α_π data, without a clear corresponding peak in the α_0 data. In Ref. [31], a bump at slightly larger energies is seen also in the ^{19}F$(p, \alpha_0)^{16}$O differential cross section at backward angles. In agreement with Refs. [31,34], this resonant behavior is attributed to the 1^- state in ^{20}Ne at $E_x = 14.417$ MeV (in our data, 14.351 MeV). Our analysis indicates a total width $\Gamma_{\text{tot}} \simeq 151$ keV, not very far from the 76-keV value quoted in Ref. [31] and the 86-keV value of Ref. [1]. Furthermore, the partial width $\Gamma_{p_0} \simeq 1.0$ keV here reported is in agreement with the upper limit of 4 keV quoted in Ref. [31]. The relatively low value of the Γ_{α_0} partial width could perhaps explain why this state is not reported in the analysis of the $\alpha + {}^{16}$O elastic scattering data of Ref. [47]. The second peak in the α_π data, centered at $E_{\text{c.m.}} \approx 1.64$ MeV,

corresponds to a very pronounced peak in the α_0 channel at the same energy. This peak is due to a 0^+ state at $E_x = 14.466$ MeV [31,34], having a dominant Γ_{α_0} partial width (about 64 keV) and also a sizable Γ_{p_0} proton width (about 7 keV). The total width values reported in the literature are 83 [34], 86 [31], and 141 keV [33]; our value is 96 keV. The partial width values here quoted are similar to the ones of Ref. [34] and the $\Gamma_{p_0} = 7$ keV proton width is not too far from the 27.1-keV width reported in Ref. [7], while it is much smaller than the 68-keV value of Ref. [31]. The use of partial width values reported in Ref. [31] will lead to a poorer description of the marked dip seen at $E_{\text{c.m.}} \simeq 1.58$ MeV in the α_π data.

The third peak seen in the α_π data, at $E_{\text{c.m.}} \approx 1.78$ MeV, has a twin structure also in the α_0 channel at very close energies. Such maxima are due to the 14.596-MeV 1^- state. The total width obtained from the present analysis is $\Gamma_{\text{tot}} = 287$ keV, while in the literature contrasting values are reported: 95 keV in Ref. [31], 125 keV in Ref. [33], and 162 keV in Ref. [1] (Table 20.28). The proton partial width here obtained (9.8 keV) is slightly larger than the upper limit of 5.5 keV reported in Ref. [31], while the branching ratios quoted in Ref. [31] (i.e., $\frac{\Gamma_{\alpha_0}}{\Gamma_{\text{tot}}} \simeq 0.65$ and $\frac{\Gamma_{\alpha_\pi}}{\Gamma_{\text{tot}}} \simeq 0.28$) are similar to the present ones (i.e., $\frac{\Gamma_{\alpha_0}}{\Gamma_{\text{tot}}} \simeq 0.74$ and $\frac{\Gamma_{\alpha_\pi}}{\Gamma_{\text{tot}}} \simeq 0.23$). The interference between this state and neighboring ones explains the deep minimum seen at $E_{\text{c.m.}} \simeq 1.69$ MeV in the α_π data. In $\alpha + {}^{16}$O elastic scattering data, a 1^- state at 14.58 MeV has been reported ($\Gamma_{\text{tot}} = 139 \pm 50$ keV), close lying to a broader 4^+ state [47]. New experiments in this energy region could perhaps help to solve such unclear situation. Another 0^+ state at $\simeq$14.65 MeV has been reported in the $p+{}^{19}$F elastic scattering analysis in Ref. [31]. Its inclusion in the present level scheme, leading to a pronounced interference with the close-lying 0^+ state at 14.466 MeV, is important to improve the quality of the fit of α_0 and α_π data in the region $E_{\text{c.m.}} \approx 1.8$ MeV. The total width of this state is larger than the one reported in Ref. [31], while the proton width is similar.

E. Resonances in the $E_{\text{c.m.}} = 1.9$–3.5 MeV region

The first part of this energy region feels the influence of several excited states of ^{20}Ne, but uncertainty are still persisting also because of the different behavior of the data sets from Refs. [13] and [33]. To try to clarify the situation, we decided to include in the R-matrix fit also some angular distributions at $E_{\text{c.m.}} = 1.96$–2.07 MeV (corresponding to $E_{\text{lab}} = 2.06$–2.18 MeV) for the α_0 and α_π channels taken from Ref. [13]. The best fit of all the data set here included is obtained with the following level scheme. First, a 1^- state is needed at 14.809 MeV, with $\Gamma_{\text{tot}} \approx 94$ keV. It is perhaps linked to the 1^- state reported at 14.773 MeV in Ref. [31] by analyzing $p + {}^{19}$F elastic scattering data. The partial width here reported are anyway different from the ones of Ref. [31]. The inclusion of such a state, with a large Γ_{α_π} partial width is needed to reproduce the shape and absolute values of α_π angular distributions in the $E_{\text{c.m.}} \approx 2$ MeV region. If such a state is not included, the trend of experimental angular distributions is not reproduced, as shown by dashed lines in Fig. 5. The small partial width for the α_0 channel could explain why this state was not reported in the analysis of $\alpha + {}^{16}$O elastic scattering data [47].

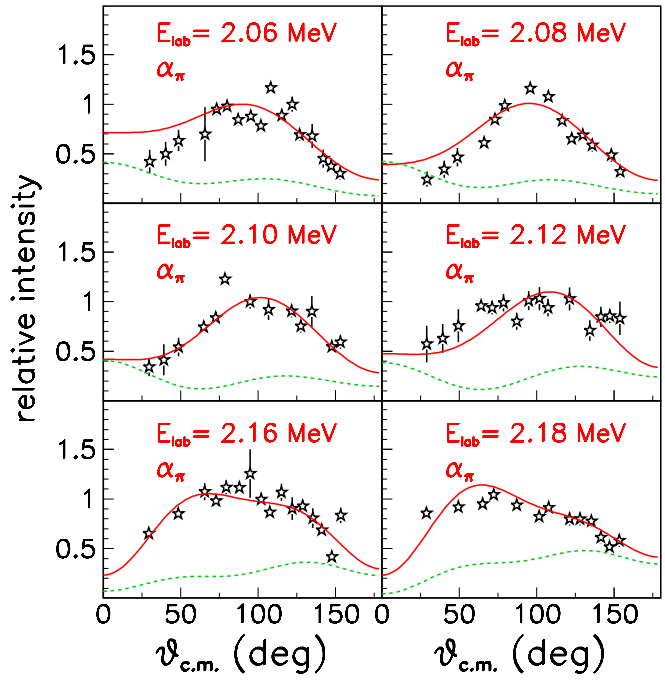

FIG. 5. Angular distributions (relative to 90°) of the ^{19}F$(p,\alpha_\pi)^{16}$O reaction at $E_{\text{lab}} = 2.06$, 2.08, 2.10, 2.12, 2.16, and 2.18 MeV. Open stars: experimental data taken from Refs. [13]. Red solid line: R-matrix fit of data, as discussed in the text. Green dashed line: R-matrix fit without the 14.809-MeV state, scaled by arbitrary factors for clarity reasons.

The second natural-parity state contributing to data in this energy region is a 4^+ state at 14.844 MeV, $\Gamma_{\text{tot}} = 139$ keV. This state was reported in the literature [33] (as 4^+) in the analysis of the α_0 reaction channel. A close inspection of the excitation functions of α_0 and α_π data of Ref. [13] shows that the two maxima seen in the α_0 and α_π data at $E_{\text{lab}} \simeq 2.12$ MeV peak at slightly different values ($\approx$30-keV shift). Furthermore, the corresponding angular distributions in this energy windows show markedly different features (e.g., at $E_{\text{lab}} \simeq 2.1$–$2.18$ MeV, a deep minimum at $\approx 65°$ is seen in the α_0 data, being absent in the α_π data; see Ref. [13]). These facts lead us to include, in the level scheme, the 4^+ state at 14.844 MeV with nonvanishing width only for the p_0 and α_0 channels. The overall features of α_0 angular distributions at $E_{\text{lab}} \simeq 2.1$ MeV are reasonably reproduced, as shown in Fig. 6; considering all the problems on the existing data sets above discussed, this can be a good starting point for future investigations. It is worth noting that a tentative 4^+ state at 14.837 MeV is also reported in the analysis of $\alpha + {}^{16}$O elastic scattering data [47], even if the total and α_0 partial widths are smaller that the present ones.

Very close in energy, a 2^+ state at 14.854 MeV is needed to reproduce in the best possible way angular distributions of both α_0 and α_π data at $E_{\text{lab}} \approx 2.12$ MeV. The presence of a 4^+-2^+ sequence of states is reported also in Ref. [47]. The total width here obtained (109 keV) agrees with the

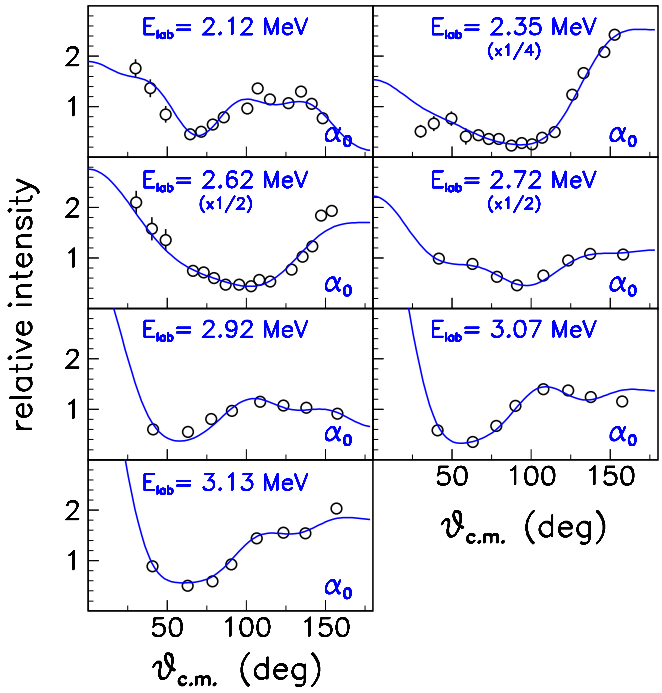

FIG. 6. Angular distributions (relative to 90°) of the ^{19}F$(p,\alpha_0)^{16}$O reaction at $E_{\rm lab} = 2.12$, 2.35, 2.62, 2.72, 2.92, 3.07, and 3.13 MeV. Where necessary, the data have been rescaled by a factor indicated in parentheses, for clarity reasons. Open dots: experimental data taken from Refs. [13,14]. Blue solid line: *R*-matrix fit of data, as discussed in the text.

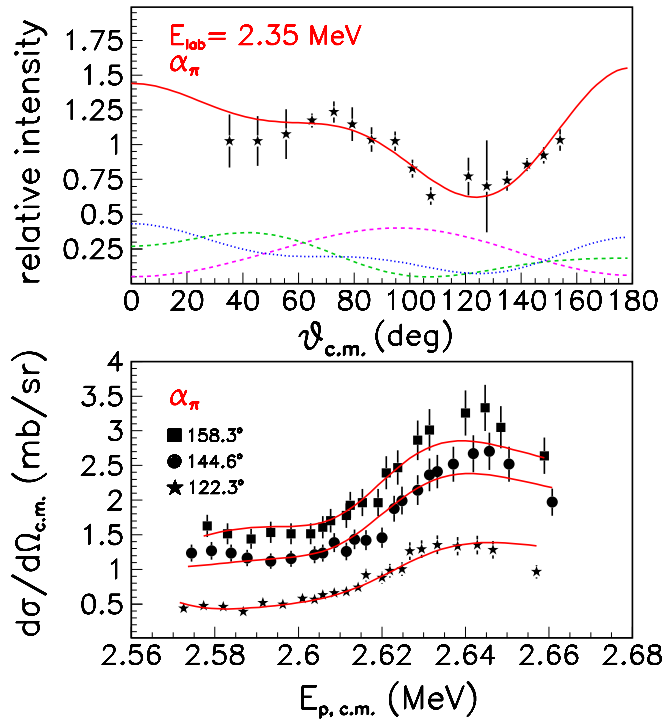

FIG. 7. (Upper panel) Angular distribution (relative to 90°) of the ^{19}F$(p,\alpha_\pi)^{16}$O reaction at $E_{\rm lab} = 2.35$ MeV. Black stars: data from Ref. [13]. Red solid line: *R*-matrix fit of data, as discussed in the text. Magenta dashed line: *R*-matrix fit without the 15.029- and 15.129-MeV states. Green dashed line: *R*-matrix fit without the 15.029-MeV state. Blue dotted line: *R*-matrix fit without the 15.129-MeV state. The last three curves are scaled by an arbitrary factor for clarity reasons. (Lower panel) Excitation functions of the ^{19}F$(p,\alpha_\pi)^{16}$O reaction in the center-of-mass energy window $E_{\rm c.m.} \simeq$ 2.57–2.67 MeV at laboratory angles of 158.3° (squares), 144.6° (circles), and 122.3° (stars). Data are derived from Ref. [18] and have been normalized respectively by 1.04, 0.91, and 1.15 factors. The red solid line is *R*-matrix fit of data, as discussed in the text.

104 ± 29 keV value reported in Ref. [47] (for the 2^+ state at 14.886 MeV), while the present Γ_{p_0} partial width is quite smaller than the ones reported in Refs. [13] and [18].

At $E_{\rm c.m.} \approx 2.08$ MeV, a peak is clearly seen in the α_π data, while no clear structure are observed in the α_0 data. In agreement with Ref. [13], we suppose the existence of a 0^+ state at 14.919 MeV with a nonzero branching only in the p_0 and α_π channels. This assumption is supported by the fact that no evidence of such a state was found in the $\alpha + {}^{16}$O elastic scattering data in Refs. [47,48]. The total and partial widths here obtained are in good agreement with the ones reported in Ref. [13].

Other structures are seen in both the α_0 and α_π channels at $E_{\rm c.m.} \approx 2.2$ MeV. The situation is complicated by the presence of a possible resonance in the α_π for which only one point (at $E_{\rm c.m.} = 2.265$ MeV) is reported in the literature [13]. In this very puzzling conditions, we tentatively reproduced the α_0 and α_π data by including two 2^+ states at 15.061 and 15.118 MeV. In principle, their interference could explain the minimum seen at $E_{\rm c.m.} = 2.233$ MeV in the α_π data; moreover, this couple of states would contribute to reproduce reasonably the angular distribution of the α_0 and α_π channels at $E_p = 2.35$ MeV ($E_{\rm c.m.} = 2.233$ MeV), as shown in Figs. 6 and 7. If we do not include one or both such states, we cannot reproduce the shape of the α_π angular distribution at this energy (see the broken lines in Fig. 7). It is interesting to observe that in the analysis of $\alpha + {}^{16}$O elastic scattering data, a couple of 2^+ states at 15.044 and 15.139 MeV has been also reported [47]. For the first state, our resonance parameters are quite similar to the ones of Ref. [47]; for the second state, our total width is larger than the one quoted in Ref. [47], while the α_0 branching ratios are similar.

At higher energy, the α_0 data become more fragmentary. Some angular distributions for the α_0 channel have been reported in Ref. [14], while excitation functions in the energy range $E_{\rm c.m.} \approx 2.56$–$2.66$ MeV were reported, at backward angles, for the α_π channel in Ref. [18]. Some of them have been included in the present analysis (allowing the presence of some small normalization factors, in the range 0.9–1.15), together with the α_0 *S*-factor data from Ref. [10].

At $E_{\rm c.m.} \approx 2.3$–2.6 MeV, a broad structure is seen in the α_0 *S*-factor data. This bump, characterized by a pronounced kurtosis, is attributed to the overlap of a 0^+ state centered at 15.297 MeV and a broader 2^+ state centered at 15.327 MeV. A 0^+ state at $\simeq$15.30 MeV was tentatively reported by Ref. [33], and also the total width here obtained (204 keV) is very close to the one reported in Refs. [33]. In Ref. [14], a state with tentative 2^+ assignment is reported at 15.34

MeV, but with a total width much smaller than the presently quoted one. Such couple of states, interfering with close-lying states, contributes to reproduce α_0 angular distributions at $E_{\rm lab} = 2.35$ and 2.92 MeV and α_π differential cross sections in the energy region shown in the lower panel of Fig. 7. The narrow structure seen at $E_{\rm c.m.} \approx 2.5$ MeV (i.e., on the top of the broad bump) is reproduced by a narrow 1^- state at 15.35 MeV; this state contributes also to reproduce the shapes of α_0 angular distributions at $E_{\rm lab} = 2.62$–3.06 MeV. Tentative 1^- states at about 15.3 MeV were reported in Refs. [14,47], having total widths of 285 and 126 keV respectively. In our case, the α_0 branching ratio is much lower than the one tentatively reported in Ref. [47].

The right tail of the bump in the α_0 data previously discussed, corresponding to the energy region $E_{\rm c.m.} \approx 2.6$–2.7 MeV, is reasonably reproduced by adding a 2^+ state at 15.419 MeV and a 3^- state at 15.451 MeV. Moreover, such a couple of states is needed to correctly reproduce the shape of angular distributions of the α_0 channel at $E_{\rm lab} = 2.62$ and 2.72 MeV, and it plays also a role in the correct reproduction of the cross-section scale of the α_π differential cross sections of Fig. 7. Signals of the existence of such a couple of states (2^+ and 3^-) at similar energies and with nearly identical total widths are found in Refs. [1,14].

A broad 2^+ state at 15.59 MeV is needed to reproduce the α_0 angular distributions at the higher energies (2.92–3.13 MeV); this state has also an influence to correctly describe the α_π excitation functions reported in Ref. [18]. In Ref. [14], a tentative 2^+ state at 15.52 MeV is reported, but with a total width much smaller than the present one. As a general consideration, it is also possible that the two broad 2^+ states at 15.327 and 15.59 MeV would mimic the presence of a d-wave direct contribution playing a role at the higher energies here explored.

Going up in energy, a 0^+ state at 15.617 MeV ($\Gamma_{\rm tot} =$ 185 keV) with a large α_π branching ratio is included mainly to reproduce the overall cross-section scale of the α_π excitation functions. Signals of the existence of such state, with a total width similar to the one here obtained (250 keV) are reported in Ref. [14], at $E_{\rm lab} = 3.0$ MeV.

The last structure that can be clearly seen in the α_0 S-factor data is an asymmetric bump centered at $E_{\rm c.m.} \approx 3$ MeV. It has been reproduced by including a 1^- state at 15.803 MeV ($\Gamma_{\rm tot} = 186$ keV) and a 3^- state at 15.821 MeV ($\Gamma_{\rm tot} =$ 205 keV). The peculiar shape of the α_0 angular distribution at $E_{\rm lab} = 3.13$ MeV is well reproduced by the presence of the 3^- state. The existence of a 3^- state at 15.88 MeV with a total width not far from the present one was suggested in Ref. [14], together with the presence of broad states with low spin at 15.7–15.9 MeV. All the remaining α_0 S-factor data is reasonably reproduced by the direct contribution discussed in the previous section, and the tiny structures seen at very high excitation energies can be attributed to statistical fluctuations.

F. Unnatural parity states contributing in $p + ^{19}$F scattering data

To describe the elastic scattering data at low energies and at backward angles (see Fig. 4), we have to include in the level scheme also unnatural parity states (Table III): Their presence is not forbidden by angular momentum and parity conservations. Because of the limited energy range of data included in the fit and considering that unnatural-parity states heavily contribute also to inelastic scattering and α_γ reactions, the present analysis of such type of states is less grounded with respect to the case of natural-parity states. It allows us to derive some partial but interesting conclusions on their spectroscopy.

The 1^+ state at 13.479 MeV ($\Gamma_{\rm tot} = 7.1$ keV) causes the evident wing at $E_{\rm c.m.} \approx 0.633$ MeV in the $p + ^{19}$F elastic scattering data at backward angles (Fig. 4); the partial widths here obtained are in good agreement with the literature ones [1,2] and also with a recent reanalysis of $p + ^{19}$F elastic scattering data [7]. At 13.675 MeV, a 2^- state has to be included in the level scheme, with a total width $\Gamma_{\rm tot} = 4.6$ keV. It is responsible for a small dip in the $p + ^{19}$F elastic scattering data at backward angles here explored at $E_{\rm c.m.} \approx 0.835$ MeV. As reported in the literature, this state has a prominent $\Gamma_{\alpha\gamma}$ width ($\simeq$82% of the total width) and $\Gamma_{p_0} \simeq 1$ keV [1]; in our analysis, we found similar results. At $E_{\rm c.m.} \approx 0.893$ MeV, $p + ^{19}$F data show a wing similar to the one seen at 0.633 MeV; in agreement with the literature, we include a 1^+ state at 13.73 MeV to reproduce such structure. The $\Gamma_{\rm tot} = 9.8$ keV here obtained is slightly larger than the values reported in Ref. [1] ($\Gamma_{\rm tot} \approx 7.7$ keV) and Ref. [7] ($\Gamma_{\rm tot} \approx 4.7$ keV).

A wing at $E_{\rm c.m.} \approx 1.07$ MeV is visible in the elastic scattering data here investigated; deviations from a pure Rutherford behavior are seen also in the old data of Ref. [41]. This feature is attributed to a narrow 1^+ state at excitation energy 13.915 MeV ($\Gamma_{\rm tot} \simeq 4.2$ keV); the obtained resonance parameters are not far from the ones reported on the literature [1,2]. Another 1^+ state with a larger width ($\Gamma_{\rm tot} \approx 74$ keV) is needed to reproduce a pronounced peak in the inelastic scattering (to the first excited state) cross section [2,42]; this state contributes to describe the shape of elastic scattering data in the $E_{\rm c.m.} \approx 1.1$–1.24 MeV region. Its resonance parameters are quite close to the ones reported in the literature [1,2].

At slightly higher energies, two consecutive minima at $E_{\rm c.m.} \simeq 1.28$, 1.3 MeV and a large wing at $E_{\rm c.m.} \simeq 1.34$ MeV characterize the elastic scattering excitation function here investigated, and this behavior is seen also in Ref. [41] for data at $\theta_{\rm c.m.} \simeq 160^\circ$. Such behavior is reproduced by a set of three states: a 2^- state at 14.126 MeV, a 2^- state at 14.151 MeV, responsible for the second minimum, and a 1^+ state at 14.195 MeV, responsible for the wing. The resonance parameters here obtained for the 14.126- and 14.151-MeV states agree well with the literature ones [1]. Concerning the 14.195-MeV state, in our work we found a total width $\Gamma_{\rm tot} \simeq$ 17.2 keV, to be compared to the values 13.9 keV of Ref. [1] and 20.1 keV of Ref. [7]. Also, the Γ_{p_0} partial width found here ($\simeq$12 keV) is intermediate with respect to the values reported by Refs. [1,7] (11.8 and 13.5 keV respectively).

A further 2^- state at 14.45 MeV is needed to explain a local minimum at $E_{\rm c.m.} \simeq 1.6$ MeV seen in the elastic scattering data. In the literature, a state with uncertain spin (1,2), negative parity, and total width $\Gamma_{\rm tot} \simeq 33 \pm 3$ keV is reported on the basis of the analysis of the ^{19}F$(p,\alpha\gamma)^{16}$O reaction [1]. Our total width $\Gamma_{\rm tot} \simeq 20$ keV is not far from

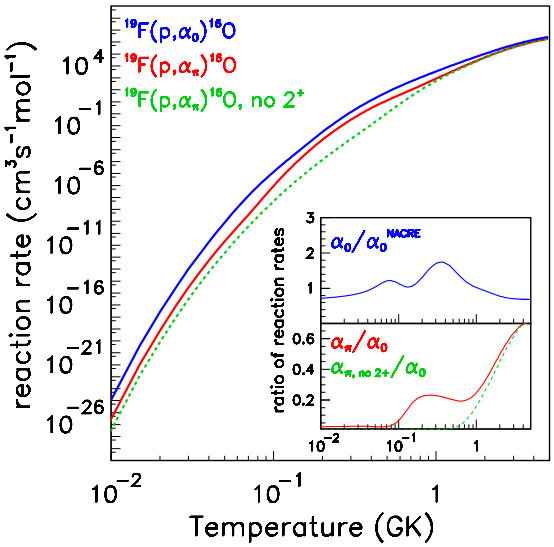

FIG. 8. Rates of the ^{19}F$(p,\alpha_0)^{16}$O (blue line) and the ^{19}F$(p,\alpha_\pi)^{16}$O (red line) reactions, as derived from the *R*-matrix analysis of data discussed in the text. The green dashed line represents the ^{19}F$(p,\alpha_\pi)^{16}$O reaction rate assuming zero α_π partial width for the 13.095-MeV state. The upper insert shows the ratio of the reaction rates for the ^{19}F$(p,\alpha_0)^{16}$O reaction calculated by using the present *R*-matrix analysis and the data set of NACRE [25]. The lower insert displays, as red solid line, the ratio between the presently estimated ^{19}F$(p,\alpha_\pi)^{16}$O and ^{19}F$(p,\alpha_0)^{16}$O reaction rates. The green dashed line shows the same ratio when zero α_π partial width for the 13.095-MeV state is assumed.

the literature value; the large value of partial width also for the inelastic channel would be in agreement with the presence of a corresponding pronounced peak in the inelastic scattering cross section [42]. Finally, a broad 1^+ state ($\Gamma_{\rm tot} \approx 220$ keV) at 14.71 MeV is (tentatively) added to the level scheme to reproduce the absolute value of the highest energy part of cross section ($E_{\rm c.m.} \simeq 1.4$–1.7 MeV). After all, at $E_{\rm lab} \approx 1.9$ MeV, Ref. [42] reports the presence of a broad maximum in the inelastic scattering cross section, while Ref. [13] show the presence of a broad bump in the $E_{\rm lab} \approx 1.8$–2 MeV region for the ^{19}F$(p,\alpha_{1,2,3})^{16}$O reaction cross section: Such findings could qualitatively justify the presence of the 14.71-MeV broad state. Furthermore, the existence of a 1^+ state at 14.699 MeV ($\Gamma_{\rm tot} = 38 \pm 10$ keV), close to a broad 1^- state at 14.776 MeV ($\Gamma_{\rm tot} = 114 \pm 19$ keV), was suggested in the literature [1,7,31]. It is possible that our tentative state at 14.71 MeV is linked to the previously reported one at 14.699 MeV, but only a new analysis including elastic scattering data in a broader energy range and reliable cross-section data for the p_1, p_2, and $\alpha\gamma$ reaction channels would help to solve the ambiguities present in the spectroscopy of unnatural-parity states at high excitation energies.

IV. REVISION OF THE $^{19}F(p,\alpha_0)^{16}O$ AND $^{19}F(p,\alpha_\pi)^{16}O$ REACTION RATES

The building of a coherent database for the ^{19}F$(p,\alpha_\pi)^{16}$O *S* factor in a quite large energy domain (see Fig. 3) and a better description of the direct component of the ^{19}F$(p,\alpha_0)^{16}$O *S* factor allow us to make some new estimates of the rate of such reactions in a temperature range of interest for the fluorine nucleosynthesis in AGB stars [58,59]. In particular, for the ^{19}F$(p,\alpha_\pi)^{16}$O case, the presence of a nonvanishing α_π partial width for the broad 2^+ state at 13.095 MeV, reported in the literature [49], can increase noticeably the *S*-factor value in the low-energy region $E_{\rm c.m.} \approx 0.2$ MeV, as discussed in Sec. III and clearly visible in Fig. 3.

Using the *R*-matrix calculations of the cross-section data, we re-estimated the rate of the two reactions ^{19}F$(p,\alpha_0)^{16}$O and ^{19}F$(p,\alpha_\pi)^{16}$O, as reported in Fig. 8 (blue and red lines) and in Table IV. The case of assuming a vanishing α_π partial width for the 13.095-MeV state is shown as green dashed line for comparison. Similar to what was discussed in Refs. [9,10], a conservative error of 20% is attributed to the present reaction rates. Concerning the ^{19}F$(p,\alpha_0)^{16}$O reaction rate, its ratio with an analogous calculation performed with

TABLE IV. Rates of the ^{19}F$(p,\alpha_0)^{16}$O and ^{19}F$(p,\alpha_\pi)^{16}$O reactions determined with the present *R*-matrix analysis of data, as a function of the temperature in GK (T_9).

T_9	Rate α_0 (cm^3 s^{-1} mol^{-1})	Rate α_π (cm^3 s^{-1} mol^{-1})
0.005	1.86×10^{-33}	4.81×10^{-37}
0.01	1.13×10^{-24}	2.92×10^{-26}
0.02	2.63×10^{-17}	7.32×10^{-19}
0.03	9.99×10^{-14}	2.88×10^{-15}
0.04	1.86×10^{-11}	5.27×10^{-13}
0.05	7.91×10^{-10}	2.06×10^{-11}
0.06	1.39×10^{-8}	3.37×10^{-10}
0.07	1.34×10^{-7}	3.51×10^{-9}
0.08	8.33×10^{-7}	2.82×10^{-8}
0.09	3.77×10^{-6}	1.79×10^{-7}
0.1	1.35×10^{-5}	9.01×10^{-7}
0.12	1.10×10^{-4}	1.26×10^{-5}
0.14	6.11×10^{-4}	9.85×10^{-5}
0.16	2.67×10^{-3}	5.18×10^{-4}
0.18	9.60×10^{-3}	2.05×10^{-3}
0.2	2.93×10^{-2}	6.56×10^{-3}
0.3	1.40×10^{0}	3.21×10^{-1}
0.4	1.38×10^{1}	2.97×10^{0}
0.5	6.45×10^{1}	1.30×10^{1}
0.6	2.01×10^{2}	3.89×10^{1}
0.7	4.93×10^{2}	9.65×10^{1}
0.8	1.04×10^{3}	2.15×10^{2}
0.9	1.97×10^{3}	4.43×10^{2}
1	3.45×10^{3}	8.54×10^{2}
1.2	8.82×10^{3}	2.65×10^{3}
1.4	1.90×10^{4}	6.77×10^{3}
1.6	3.64×10^{4}	1.49×10^{4}
1.8	6.39×10^{4}	2.91×10^{4}
2	1.04×10^{5}	5.20×10^{4}
2.5	2.80×10^{5}	1.62×10^{5}
3	5.80×10^{5}	3.69×10^{5}
3.5	1.00×10^{6}	6.75×10^{5}
4	1.53×10^{6}	1.06×10^{6}
4.5	2.13×10^{6}	1.50×10^{6}
5	2.77×10^{6}	1.97×10^{6}

the corresponding NACRE data is shown as the blue line in the inset of Fig. 8. Within the errors, such ratio is in agreement with the recent findings of Refs. [9,10,60], even if the different description of the direct contributions at low energies, discussed in the present work, is responsible for a reduction of the reaction rate at the lowermost temperatures ($T \lesssim 0.1$ GK). Furthermore, as discussed in the previous section, the *R*-matrix calculation slightly underestimates the ^{19}F$(p,\alpha_0)^{16}$O experimental data in the $E_{\rm c.m.} \approx 0.4$–0.6 MeV region, and this would correspondingly reflect in a reaction rate slightly lower than the ones calculated in Refs. [9,10,60].

As a second, and more important, point for reflection, it is evident that, in the temperature range $T \approx 0.1$–1 GK, the presence of a nonvanishing α_π partial width for the 13.095-MeV state highly enhances the ^{19}F$(p,\alpha_\pi)^{16}$O reaction rate. This effect is more evident in the inset of Fig. 8, where the ratio between ^{19}F$(p,\alpha_\pi)^{16}$O and ^{19}F(p, $\alpha_0)^{16}$O reaction rates is shown with red solid and green dashed lines. The first case refers to the presence of $\Gamma_{\alpha_\pi} = 43.7$ keV for the 13.095-MeV state, while the second case refers to zero α_π partial width for such a state. As clearly seen, in the first case the α_π reaction rate at $T \approx 0.2$–0.5 GK can reach up to ≈25% of the α_0 reaction rate and should not be neglected in the estimate of the total ^{19}F$(p,\alpha)^{16}$O reaction rate. On the other hand, for the second case (green dashed line), at $T < 0.5$ GK, the reaction rate for the ^{19}F$(p,\alpha_\pi)^{16}$O would be negligible with respect to the ^{19}F$(p,\alpha_0)^{16}$O.

It is interesting to emphasize that in NACRE [25], the low-energy part ($E_{\rm c.m.} < 0.4$ MeV) of the ^{19}F$(p,\alpha_\pi)^{16}$O S factor is described with an almost constant nonresonant approximation $S(E) \approx 1.2$ MeV b, in contrast with the present estimates based on the spectroscopy of the 13.095-MeV state. At this point, it would be extremely interesting to perform a new measurement of the ^{19}F$(p,\alpha_\pi)^{16}$O near 0.25 MeV to confirm our predictions.

V. CONCLUSIONS

In this work, we discussed a comprehensive reinvestigation of the spectroscopy of low-spin natural-parity states in the self-conjugate nucleus ^{20}Ne, in a very broad excitation energy window ($E_x \approx 13$–16 MeV) above the proton separation energy. This analysis was mainly based on the study of excitation functions, angular distributions, and angle-integrated cross sections of the two reactions ^{19}F$(p,\alpha_0)^{16}$O and ^{19}F$(p,\alpha_\pi)^{16}$O at low bombarding energies. For the ^{19}F$(p,\alpha_0)^{16}$O case, we benefited of the accurate reanalysis of all the experimental data available in the literature discussed in Ref. [10], while for the ^{19}F$(p,\alpha_\pi)^{16}$O case we built a new dataset by using the data available in the literature and making detailed comparisons between them. Data on the elastic scattering of $p+^{19}$F at low energies and backward angles were also used to estimate in the best possible way the partial widths associated with the various reaction channels. We performed a simultaneous *R*-matrix fit of a large body of data involving such reaction channels; for all the cases where contrasting assignments are reported in the literature, we performed a dedicated analysis with the aim of solving such ambiguities. As a result of the analysis, we obtained an improved spectroscopy of excited states of ^{20}Ne at high energies, which can serve as a solid basis for further speculations on its structure. The inclusion in the data set of high-energy points allows us to obtain a coherent description of the direct contribution in the ^{19}F$(p,\alpha_0)^{16}$O cross section, that would affect also the estimate of the reaction rate at low temperatures. From the spectroscopy of the 13.095-MeV state, we suggest that it can play a non-negligible role in the determination of the ^{19}F$(p,\alpha_\pi)^{16}$O reaction rate in the temperature region $T \approx 0.2$–0.5 GK. New dedicated experiments at proton bombarding energies around 0.28 MeV would be crucial to confirm, with a direct measurement, this finding.

ACKNOWLEDGMENTS

We acknowledge all the members of the University of Naples team who, about fifty years ago, started to investigate these reactions at low energies. In particular, I.L., D.D.A., G.S., and M.V. are indebted to P. Cuzzocrea, E. Perillo, and E. Rosato (deceased) (Napoli) for useful discussions, comments, and suggestions about the subject of this paper. I.L. thanks R. J. DeBoer (Notre Dame) for discussions on the *R*-matrix code and M. La Cognata (LNS Catania) for discussions on the subject of this paper. The work of I.L. has been partly supported by an INFN-SyLiNuRe grant. J.-J.H. was financially supported by the National Natural Science Foundation of China (Grants No. 11825504 and No. 11490562) and the Major State Basic Research Development Program of China (Grant No. 2016YFA0400503).

[1] D. R. Tilley, C. M. Cheves, J. H. Kelley, S. Raman, and H. R. Weller, Nucl. Phys. A **636**, 249 (1998).
[2] C. A. Barnes, Phys. Rev. **97**, 1226 (1955).
[3] A. Couture, M. Beard, M. Couder, J. Görres, L. Lamm, P. J. Leblanc, H. Y. Lee, S. O'Brien, A. Palumbo, E. Stech *et al.*, Phys. Rev. C **77**, 015802 (2008).
[4] W. E. Burcham and S. Devons, Proc. R. Soc. London, Ser. A **173**, 555 (1939).
[5] A. Isoya, Nucl. Phys. A **7**, 126 (1958).
[6] V. Paneta, A. Kafkarkou, M. Kokkoris, and A. Lagoyannis, Nucl. Instrum. Methods Phys. Res. B **288**, 53 (2012).
[7] V. Paneta, A. Gurbich, and M. Kokkoris, Nucl. Instrum. Methods Phys. Res. B **371**, 54 (2016).
[8] I. Lombardo *et al.*, J. Phys. G **40**, 125102 (2013).
[9] I. Lombardo *et al.*, Phys. Lett. B **748**, 178 (2015).
[10] J.-J. He, I. Lombardo, D. Dell'Aquila, Yi Xu, L.-Y. Zhang, and W.-P. Liu, Chin. Phys. C **42**, 15001 (2018).
[11] I. Lombardo *et al.*, Bull. Russ. Acad. Sci. Phys. **78**, 1093 (2014).
[12] K. L. Warsh, G. M. Temmer, and H. R. Blieden, Phys. Rev. **131**, 1690 (1963).
[13] P. Cuzzocrea *et al.*, Lett. Nuovo Cim. **28**, 515 (1980).

[14] G. Breuer and L. Jahnke, Zeitschr. Nat. A **19**, 471 (1964).
[15] S. Devons, G. Goldring, and G. R. Lindsey, Proc. Phys. Soc. A **67**, 134 (1954).
[16] R. Caracciolo *et al.*, Lett. Nuovo Cim. **11**, 33 (1974).
[17] P. Cuzzocrea, A. De Rosa, G. Inglima, E. Perillo, E. Rosato, M. Sandoli, and G. Spadaccini, INFN Report INFN/BE-80/5, 1 (1980).
[18] S. Ouichaoui, H. Beaumevieille, N. Bendjaballah, and A. Genoux-Lubain, Nuovo Cim. A **94**, 133 (1986).
[19] K. L. Warsh and S. Edwards, Nucl. Phys. A **65**, 382 (1965).
[20] G. M. Temmer, Phys. Rev. Lett. **12**, 330 (1964).
[21] P. Guazzoni, I. Iori, S. Micheletti, N. Molho, M. Pignanelli, and G. Tagliaferri, Nuovo Cim. A **67**, 407 (1970).
[22] H. Herndl, H. Abele, G. Staudt, B. Bach, K. Grün, H. Scsribany, H. Oberhummer, and G. Raimann, Phys. Rev. C **44**, R952 (1991).
[23] Y. Yamashita and Y. Kudo, Prog. Theor. Phys. **90**, 1303 (1993).
[24] M. Wiescher, J. Görres, and H. Schatz, J. Phys. G Nucl. Phys. **25**, R133 (1999).
[25] C. Angulo *et al.*, Nucl. Phys. A **656**, 3 (1999).
[26] W. A. Ranken, T. W. Bonner, and J. H. McCrary, Phys. Rev. **109**, 1646 (1958).
[27] J. F. Streib, W. A. Fowler, and C. C. Lauritsen, Phys. Rev. **59**, 253 (1941).
[28] G. C. Phillips and N. P. Heydenburg, Phys. Rev. **83**, 184 (1951).
[29] A. Isoya, K. Goto, and T. Momota, J. Phys. Soc. Japan **11**, 899 (1956).
[30] C. Y. Chao, A. V. Tollestrup, W. A. Fowler, and C. C. Lauritsen, Phys. Rev. **79**, 108 (1950).
[31] S. Ouichaoui, H. Beaumevieille, N. Bendjaballah, C. Chami, A. Dauchy, B. Chambon, D. Drain, and C. Pastor, Nuovo Cim. A **86**, 170 (1985).
[32] K. M. Subotić, R. Ostogić, and B. Z. Stepančić, Nucl. Phys. A **331**, 491 (1979).
[33] R. L. Clarke and E. B. Paul, Can. J. Phys. **35**, 155 (1957).
[34] A. De Rosa, E. Perillo, P. Cuzzocrea, G. Inglima, E. Rosato, M. Sandoli, and G. Spadaccini, Nuovo Cim. A **44**, 433 (1978).
[35] R. A. Ricci, Nucl. Instrum. Methods Phys. Res. A **328**, 355 (1993).
[36] L. Campajola, A. Brondi, A. D'Onofrio, G. Gialanella, M. Romano, F. Terrasi, C. Tuniz, C. Azzi, and S. Improta, Nucl. Instrum. Methods Phys. Res. B **29**, 129 (1987).
[37] I. Lombardo *et al.*, J. Phys. G. **43**, 45109 (2016).
[38] I. Lombardo *et al.*, J. Phys.: Conf. Ser. **569**, 012068 (2014).
[39] I. Lombardo, D. Dell'Aquila, G. Spadaccini, G. Verde, and M. Vigilante, Phys. Rev. C **97**, 034320 (2018).
[40] I. Lombardo *et al.*, Nucl. Instrum. Meth. Phys. Res. B **302**, 19 (2013).
[41] T. S. Webb, F. B. Hagedorn, W. A. Fowler, and C. C. Lauritsen, Phys. Rev. **99**, 138 (1955).
[42] M. A. Chaudhri, Radiat. Effects **94**, 145 (1986).
[43] Ph. Gorodetzky *et al.*, J. Phys. C **11–12**, 197 (1971).
[44] A. Arima, V. Gillet, and J. Ginocchio, Phys. Rev. Lett. **25**, 1043 (1970).
[45] R. Middleton, J. D. Garrett, and H. T. Fortune, Phys. Rev. Lett. **27**, 950 (1971).
[46] D. K. Nauruzbayev, V. Z. Goldberg, A. K. Nurmukhanbetova, M. S. Golovkov, A. Volya, G. V. Rogachev, and R. E. Tribble, Phys. Rev. C **96**, 014322 (2017).
[47] G. Caskey, Phys. Rev. C **31**, 717 (1985).
[48] M. K. Mehta, W. E. Hunt, and R. H. Davis, Phys. Rev. **160**, 791 (1967).
[49] C. M. Laymon, K. D. Brown, and D. P. Balamuth, Phys. Rev. C **45**, 576 (1992).
[50] R. E. Azuma *et al.*, Phys. Rev. C **81**, 045805 (2010).
[51] R. J. deBoer, D. W. Bardayan, J. Görres, P. J. LeBlanc, K. V. Manukyan, M. T. Moran, K. Smith, W. Tan, E. Uberseder, M. Wiescher *et al.*, Phys. Rev. C **91**, 045804 (2015).
[52] M. Wiescher, R. J. de Boer, J. Görres, and R. E. Azuma, Phys. Rev. C **95**, 044617 (2017).
[53] M. Freer, J. D. Malcolm, N. L. Achouri, N. I. Ashwood, D. W. Bardayan, S. M. Brown, W. N. Catford, K. A. Chipps, J. Cizewski, N. Curtis *et al.*, Phys. Rev. C **90**, 054324 (2014).
[54] C. R. Brune, Phys. Rev. C **66**, 044611 (2002).
[55] G. Breuer, Z. Phys. **154**, 339 (1959).
[56] J. Kuperus, P. W. M. Glaudemans, and P. M. Endt, Physica **29**, 1281 (1963).
[57] C. Spitaleri, S. M. R. Puglia, M. La Cognata, L. Lamia, S. Cherubini, A. Cvetinović, G. D'Agata, M. Gulino, G. L. Guardo, I. Indelicato *et al.*, Phys. Rev. C **95**, 035801 (2017).
[58] M. La Cognata, A. M. Mukhamedzhanov, C. Spitaleri, I. Indelicato, M. Aliotta, V. Burjan, S. Cherubini, A. Coc, M. Gulino, Z. Hons *et al.*, Astr. Phys. J. Lett. **739**, L54 (2011).
[59] M. La Cognata, S. Palmerini, C. Spitaleri, I. Indelicato, A. M. Mukhamedzhanov, I. Lombardo, and O. Trippella, Astr. Phys. J. **805**, 128 (2015).
[60] I. Indelicato, M. La Cognata, C. Spitaleri, V. Burjan, S. Cherubini, M. Gulino, S. Hayakawa, Z. Hons, V. Kroha, L. Lamia *et al.*, Astr. Phys. J. **845**, 19 (2017).
[61] W. Liu, Z. Li, J. He, X. Tang, G. Lian, Z. An, J. Chang, H. Chen, Q. Chen, X. Chen *et al.*, Sci. China Phys., Mech. Astron. **59**, 5785 (2016).
[62] J. He, S. Xu, S. Ma, J. Hu, L. Zhang, C. Fu, N. Zhang, G. Lian, J. Su, Y. Li *et al.*, Sci. China Phys., Mech. Astron. **59**, 5797 (2016).
[63] E. F. Garman, Ph.D. thesis, University of Oxford, Oxford, UK, 1980 (unpublished).
[64] D. Dieumegard, B. Maurel, and G. Amsel, Nucl. Instrum. Methods **168**, 93 (1980).